

# Enhancing capabilities of Atomic Force Microscopy by tip motion harmonics analysis

S. BABICZ<sup>1\*</sup>, J. SMULKO<sup>1</sup>, and A. ZIELIŃSKI<sup>2</sup>

<sup>1</sup> Faculty of Electronics, Telecommunications and Informatics, Department of Metrology and Optoelectronics,  
Gdansk University of Technology, 11/12 G. Narutowicza St., 80-233 Gdansk, Poland

<sup>2</sup> Chemical Faculty, Department of Electrochemistry, Corrosion and Materials Engineering, Gdansk University of Technology,  
11/12 G. Narutowicza St., 80-233 Gdansk, Poland

**Abstract.** Motion of a tip used in an atomic force microscope can be described by the Lennard-Jones potential, approximated by the van der Waals force in a long-range interaction. Here we present a general framework of approximation of the tip motion by adding three terms of Taylor series what results in non-zero harmonics in an output signal. We have worked out a measurement system which allows recording of an excitation tip signal and its non-linear response. The first studies of spectrum showed that presence of the second and the third harmonics in cantilever vibrations may be observed and used as a new method of the investigated samples characterization.

**Key words:** atomic force microscopy, harmonics, van der Waals force.

## 1. Introduction

Since the 20th century, when the science has brought many discoveries in the field of nanotechnology, like metallic clusters, nanotubes, thin films or nanowires, a study of surface morphology and its imaging with atomic resolution has become one of the most important subjects. The breakthrough has occurred in 1980's when a series of scanning probe microscopes (SPM) were invented. The SPM defines a broad group of high sensitivity instruments used to determine chemical and biological properties of various materials. One of these microscopes, a scanning tunnelling microscope (STM), was developed by Gerd Binnig and Heinrich Rohrer (at IBM Zürich) in 1982 [1]. The inventors earned the Nobel Prize in Physics in 1986 for the discovery. The STM investigates morphology of the probe basing on the concept of quantum tunnelling. The tunnelling current is found to be proportional to the local density of surface's states, at the position of the tip. Unfortunately, this method does not allow analyzing insulators and biological materials (viruses, bacteria or DNA must by very often investigated in their natural environment).

This fact, associated with surface science, materials engineering, biochemistry and biotechnology development, prompted one of the constructors of STM, Gerd Binnig, to build another tool for microscopy research. He has invented the first atomic force microscope (AFM) [2]. The AFM illustrates more precisely topography of the sample by investigating forces between the applied tip and the sample atoms [3].

Today the AFM is a powerful, versatile and fundamental tool for visualization and studying the morphology of materials surface. Partially, atomic force microscopy is widely used to research materials as well as mechanical properties of nanostructures [4]. Moreover, the AFM can also be used to

measure force-versus-distance curves [5]. Such curves, briefly called force curves, provide valuable information on local material properties like adhesion, hardness or elasticity.

A few different methods of sample testing were proposed to improve information recognized by the moving tip (e.g. image resolution) [6–10], but there is still a continuous need to improve quality of the collected data. In this paper we propose to utilize information about non-linearity of the vibrating tip which depends on non-linear force between the sample and the vibrating tip. The non-linearity is connected with topography substructures and different physical properties of the investigated materials. For non-uniform materials new information could be revealed by higher harmonics. In homogenous materials we can expect improvement in image resolution at edges of the identified substructures.

Such attempts were done by various teams [11–14]. Some measurement solutions require specialized microscopic probes [11] or are limited to an image of the selected harmonic [12–14]. The presented solution is more general and determines images for a few different harmonics.

Practical applications of the presented method need careful measurements of tip vibrations to determine intensity of the second and the third harmonics. Thus, we present a general framework for harmonics recording and analyzing using exemplary AFM device. This method of AFM investigations may significantly enhance contemporary applied methods of surface investigations and gives additional information for better characterization of the tested samples.

## 2. Principles of Dynamic Force Microscopy

The AFM image is generated by recording signals related to a force which occurs between the vibrating cantilever and the

\*e-mail: sylwia.babicz@eti.pg.gda.pl

atoms of the investigated sample (Fig. 1) in the  $x$  and  $y$  directions. The principle of operation is shown in Fig. 2. A sharp tip is attached to the free end of a flexible cantilever placed in a close proximity of the tested sample. At another end of the cantilever, a piezo is attached to induce cantilever vibrations of amplitude  $A$ , and hence the tip at the resonant frequency  $f_0$  of this mechanical object. During scanning, a sharp silicon (or silicon nitride) tip moves over the sample surface. As a result of the existing tip-surface forces, the cantilever bends. The optical method is the most common approach to detect the deflections from the tip mean position [15]. It comprises the laser focused beam on the back side of the cantilever which is measured after reflection by a matrix of photodiodes. A feedback loop is employed within the AFM control unit to keep constant the acting force on the AFM tip. Depending on the chosen measurement technique, the AFM examines the force-distance dependence in different ranges of the Lennard-Jones function, which describes in general forces between the tip and the surface atoms. The AFM techniques of measurement can be used in one of three different working modes (Fig. 3): contact mode, tapping mode and non-contact mode [16]. The presented results are obtained for the non-contact mode when the tip is attracted by the sample at any moment.

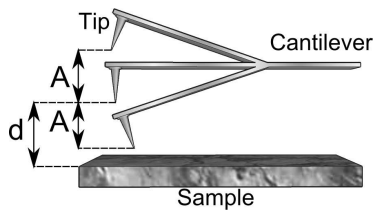


Fig. 1. Scheme of the relevant spatial distance in non-contact mode of AFM between the investigated sample and the tip

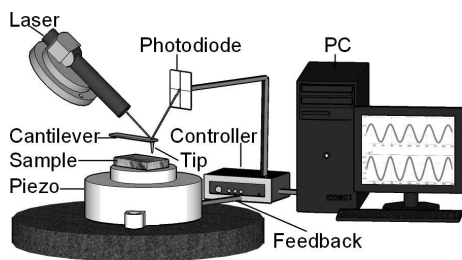


Fig. 2. The schematic setup of AFM

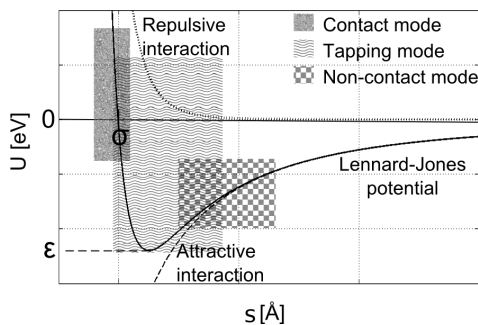


Fig. 3. Sketch of a typical tip-sample potential

The forces between two atoms can be approximated by Lennard-Jones potential energy function [17, 18]:

$$U(s) = 4\epsilon \left( \frac{\sigma^{12}}{s^{12}} - \frac{\sigma^6}{s^6} \right), \quad (1)$$

where  $s$  – tip-sample distance,  $\epsilon$  – the depth of the potential well,  $\sigma$  – the finite distance at which the inter-particle potential is zero.

The potential function is shown in Fig. 3. Lennard-Jones potential (solid line) depends on the distance between tip and sample and is a total potential of the repulsive (dotted line) and successive interactions (dashed line). The force induced by the Lennard-Jones potential between a tip and a sample is its derivative:

$$F(s) = -\frac{\partial U(s)}{\partial s} = \frac{24\epsilon}{\sigma} \left( 2\frac{\sigma^{13}}{s^{13}} - \frac{\sigma^7}{s^7} \right). \quad (2)$$

The interaction between tip and sample causes a shift of the resonance frequency of the cantilever which can be detected and used for image formation [17–20]. This frequency shift is associated with a gradient of the tip-sample interaction force. The reason of frequency shift is easily described by Fig. 4. Normally, the tip moves in a parabolic potential (dotted line). The same situation may be observed if the tip is far away from sample ( $s \gg d + A$ ). In such a case the tip’s oscillations are harmonic and its motion is sinusoidal. Thus, the resonance frequency is given by eigenfrequency  $f_0$  of the cantilever. If the condition  $s \ll d$  is fulfilled the influence of the Lennard-Jones potential (dashed line) is stronger and the effective potential (solid line) differs from the original parabolic potential by showing an asymmetric shape [21].

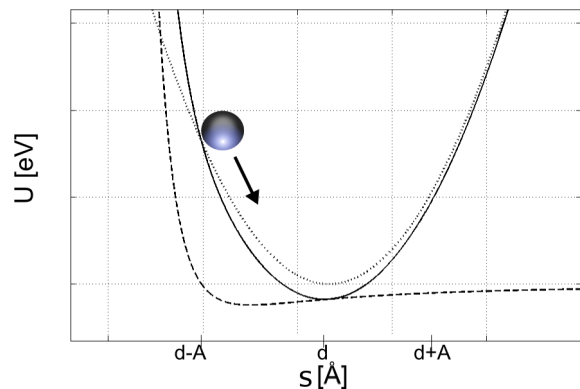


Fig. 4. Graph illustrating the reason for the frequency shift [18]

### 3. Theory of non-linearities in tip motion

The theory of non-linearities focuses on non-contact mode, where the non-linearities are less visible but can be predicted by the presented theoretical model.

As it is shown in Figs. 3 and 4, the Lennard-Jones potential has the strongest influence in a short-range distance such as  $d < 6 \text{ \AA}$ . As the model for a long-range force between the tip and the sample only attractive forces should be chosen. This takes place in a non-contact mode. The attractive forces are described by the van der Waals equation:

$$F(s) = -\frac{A_H R}{6s^2}, \quad (3)$$

where  $A_H$  – Hamaker constant,  $R$  – the tip radius.

The applied van der Waals force is an approximation of the derivative of the Lennard-Jones potential at non-contact mode applied in the presented data when only high-range forces are considered. At typical measurement conditions, the distance between the tip and the sample cannot be smaller than  $100 \mu\text{m}$  without cooling down and placing the sample in vacuum.

Equation (3) can be used to describe motion of the tip [22]:

$$F(s) = -\frac{A_H R}{6s^2} \\ = m_{eff} \frac{\partial^2 s}{\partial t^2} + \frac{m_{eff} f_0}{Q} \frac{\partial s}{\partial t} + k(s - d) - kA \cos(f_0 t), \quad (4)$$

where  $m_{eff}$  – effective mass of the cantilever,  $Q$  – a cantilever quality factor ( $Q$  factor),  $k$  – cantilever spring constant. Effective mass of the cantilever is given by:

$$m_{eff} = \frac{k}{(2\pi f_0)^2}. \quad (5)$$

The right part of (4) may be approximated by two terms of the Taylor series:

$$F(s) = -\frac{A_H R}{6s^2} = F(d_0) \\ + \frac{\partial F(d_0)}{\partial s} (s - d_0) + \frac{\partial^2 F(d_0)}{\partial s^2} (s - d_0)^2 + \dots \quad (6)$$

where  $d_0$  – the equilibrium point which is given by the root of:

$$k(s - d) = F(s). \quad (7)$$

The presented equation predicts appearance of non-linear effects in tip motion. These non-linear components will generate higher order harmonics. There is no analytical method of solving such non-linear differential equation. We can solve (6) by applying numerical methods to determine intensities of the second and the third harmonics components, present in the assumed approximation.

The cantilever was excited in air by a clear harmonic signal. Then the spectrum of the tip oscillations exhibited a component at excitation frequency only, without any higher harmonic components. Thus, we conclude that the van der Waals force, induced by the investigated sample at non-contact mode, is responsible for the observed non-linear effects. Such information can be used to improve quality of the recorded pictures or to characterize its physical properties. Intensities of the observed harmonics should be related to the Hamaker constant which changes within area of the investigated non-uniform sample. Such relation can be established by some numerical investigations which are currently in preparation.

#### 4. Measurement system and experimental data

Measurement system is shown in Fig. 5. The AFM system NTEGRA Prima produced by NT-MDT was used as the AFM. We also employed National Instruments USB-6356 acquisition card to collect signals and program written in LabView to record them.

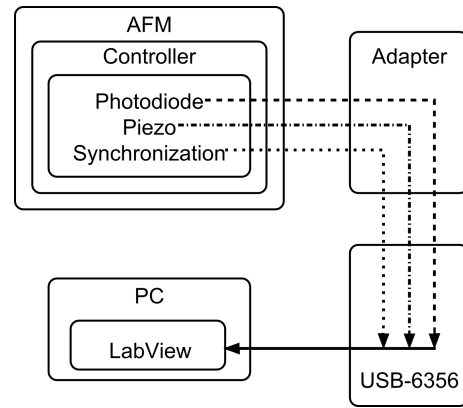


Fig. 5. Block diagram of the AFM measurement system

A fresh tip, type NSG01 produced by NT-MDT, was applied to perform experiment. During traditional scanning and creating image of the sample’s surface we recorded three channels: the harmonic signal from a piezo which excites the cantilever, an output signal of the cantilever vibrations from a photodiode and a synchronization signal. The sampling frequency was set to 1.25 MHz to observe the second and the third harmonics because of the cantilever resonance frequency was within a range of 160–180 kHz.

The first measurements were made by applying a non-contact mode, when the tip does not reach the surface and non-linear effects are less visible when compared with conditions existing in tapping mode. Firstly, we established intensity of harmonic components of the cantilever vibrating freely in air. The vibrating cantilever displayed only second harmonic component, which was three orders lower than the tip eigenfrequency  $f_o$  (Fig. 6a). The excitation signal was clearly harmonic. Thus the observed component (Fig. 6a) was caused by some non-linearity of the tip motion.

To detect the higher harmonics a lock-in amplifier was used. The lock-in amplifier was designed using the algorithm described in the literature [23–25]. In this solution the lock-in amplifier comprises a reference generator (piezo) signal and a cantilever (photodiode) output signal. The investigated system is stimulated by the reference harmonic signal. The signal from photodiode is sampled and then multiplied by the generator signal. This product is filtered by a low-pass filter to reduce noise which is not correlated with the harmonic component of the signal induced by the input reference [25]. This operation allows extraction of low-intensity higher harmonics from original output signal which includes as well noise impeding the proper analysis of the results.

As the next step, we observed signals for the same cantilever when the sapphire structure was moved closer to satisfy conditions for non-contact mode measurements. In this case, the cantilever demonstrated more intense non-linear effects which resulted in stronger second harmonic component (more than three times stronger) and appearance of the third harmonic (Fig. 6b). This proves that motion of the tip in air, without any interaction with the sample, is almost linear and an occurrence of the higher harmonics results from tip-sample interactions.

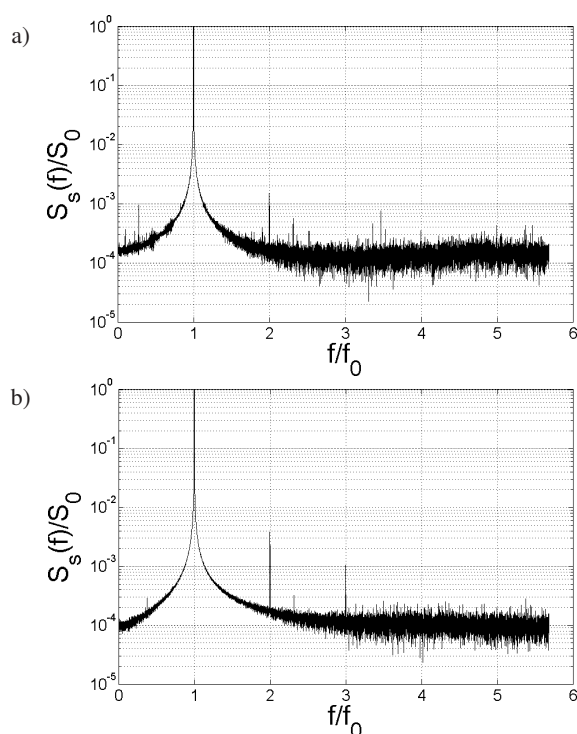


Fig. 6. Normalized spectrum  $S_s(f)$  of the cantilever vibrations: a) in air, b) in non-contact mode at vicinity of exemplary sapphire structure

The similar results in tapping-mode were observed for other samples, like ZnO structures. Additionally, when the recorded synchronizing signal was considered we were able to scan changes of the higher harmonics intensities for all pixels of the acquired surface picture. Thus, we can conclude that the present method can be successfully applied to gather more information about the investigated samples. A more detailed study is necessary to establish a way how new information should be optimally visualized in the recorded pictures.



Fig. 7. Topography of graphene observed in tapping-mode made by dedicated software (a) and image of the second harmonic component (b)

Second harmonic amplitude and topography image were simultaneously recorded on the surface of graphene. Figure 7a shows the topography made via the dedicated NOVA software. Figure 7b presents the topography image of the same fragment

of the sample made by measuring the second harmonic. Image is the result of scaling matrix containing the value of the second harmonic for each pixel by the gray map. The second harmonic image (Fig. 7b) emphasizes some elements of topographical substructures – their edges are sharper and clearly visible when compared with blurred image of topographical scans (Fig. 7a).

## 5. Conclusions

A new method of non-linear effects recognition in AFM signals has been proposed. The preliminary experimental data showed that such measurements can be effectively performed by applying data acquisition and a processing system.

The introductory theoretical considerations of non-linear effects in tip motion, caused by interaction with the sample, have been presented as well. We conclude that the equation which approximates tip motion and predicts presence of higher harmonics in movement of the oscillating tip has to be solved numerically. Further studies are currently performed for the grainy samples of non-homogenous properties, which assure different van der Waals forces on the investigated sample surface.

## REFERENCES

- [1] G. Binnig and H. Rohrer, "Scanning tunneling microscopy", *Surface Science* 126, 236–244 (1983).
- [2] G. Binnig and C.F. Quate, "Atomic force microscope", *Physical Review Letters* 56, 930–933 (1986).
- [3] R. Garcia and A. San Paulo, "Attractive and repulsive tip-sample interaction regimes in tapping-mode atomic force microscopy", *Physical Review B* 60, 4961–4967 (1999).
- [4] S. Cuenot, Ch. Frétiqny, S. Demoustier-Champagne, and B. Nysten, "Surface tension effect on the mechanical properties of nanomaterials measured by atomic force microscopy", *Physical Review B* 69, 165410 (2004).
- [5] Y. Sugimoto, P. Pou, M. Abe, P. Jelinek, R. Perez, S. Morita, and O. Custance, "Chemical identification of individual surface atoms by atomic force microscopy", *Nature* 446, 64–67 (2007).
- [6] R. Perez, Y. Stich, M. Payne, and K. Terakura, "Surface-tip interactions in noncontact atomic-force microscopy on reactive surfaces: Si(111)", *Physical Review B* 58, 10835–10849 (1998).
- [7] T. Fukuma, J.I. Kilpatrick, and S.P. Jarvis, "Phase modulation atomic force microscope with true atomic resolution", *Review of Scientific Instruments* 77, 123703 (2006).
- [8] D. Platz, E.A. Tholen, C. Hutter, A.C. von Bieren, and D.B. Haviland, "Phase imaging with intermodulation atomic force microscopy", *Ultramicroscopy* 110, 573–577 (2010).
- [9] N.F. Martínez and R. García, "Measuring phase shifts and energy dissipation with amplitude modulation atomic force microscopy", *Nanotechnology* 17 (7), S167–S172 (2006).
- [10] R. Garcia and R. Perez, "Dynamic atomic force microscopy methods", *Surface Science Reports* 47, 197–301 (2002).
- [11] A. Sikora and Ł. Bednarz, "The implementation and the performance analysis of the multi-channel software-based lock-in amplifier for the stiffness mapping with atomic force microscope (AFM)", *Bull. Pol. Ac.: Tech.* 60 (1), 83–88 (2012).



- [12] R. Hillenbrand, M. Stark, and R. Guckenberger, "Higher-harmonics generation in tapping-mode atomic-force microscopy: insights into the tip-sample interaction", *Applied Physics Letters* 76 (23), 3478–3480 (2000).
- [13] R.W. Stark, "Spectroscopy of higher harmonics in dynamic atomic force microscopy", *Nanotechnology* 15, 347–351 (2004).
- [14] R.W. Stark and W.M. Heckl, "Higher harmonics imaging in tapping-mode atomic-force microscopy", *Review Scientific Instruments* 74 (12), 5111–5114 (2003).
- [15] T. Gotszalk, P. Grabiec, and I.W. Rangelow, "Piezoresistive sensors for scanning probe microscopy", *Ultramicroscopy* 82, 39–48 (2000).
- [16] P. Eaton and P. West, "Atomic force microscopy", Oxford University Press, London, 2011.
- [17] F.J. Giessibl, "Forces and frequency shifts in atomic-resolution dynamic-force microscopy", *Physical Review B* 56, 16010–16015 (1997).
- [18] H. Ueyama, M. Ohta, Y. Sugawara, and S. Morita, "Atomically resolved InP(110) surface observed with noncontact ultrahigh vacuum atomic force microscope", *Japan Applied Physics* 61, L1086–L1088 (1995).
- [19] F.J. Giessibl, "Atomic resolution of the silicon (111)-(7X7) surface by atomic force microscopy", *Science* 67 (5194), 68–71 (1995).
- [20] R. Lüthi, E. Meyer, M. Bammerlin, A. Baratoff, T. Lehmann, L. Howald, C. Gerber, and H.J. Güntherodt, "Atomic resolution in dynamic force microscopy across steps on Si(111)7×7", *Zeitschrift für Physik B* 100, 165–167 (1996).
- [21] H. Hölscher, U.D. Schwarz, and R. Wiesendanger, "Calculation of the frequency shift in dynamic force microscopy", *Applied Surface Science* 140, 344–351 (1999).
- [22] N. Sasaki and M. Tsukada, "The relation between resonance curves and tip-surface interaction potential in noncontact atomic-force microscopy", *Japan J. Applied Physics* 37, L533–L535 (1998).
- [23] M.L. Meade, "Lock-in amplifiers: Principles and application", *IEE Electrical Measurement Series* 1, CD-ROM (1983).
- [24] J.H. Scofield, "Frequency-domain description of a lock-in amplifier", *Am. J. Physics* 66, 129–133 (1994).
- [25] M. Kotarski and J. Smulko, "Assessment of synchronic detection at low frequencies through DSP-based board and PC sound card", *XIX IMEHO World Congress Fundamental and Applied Metrology* 1, 960–963 (2009).